

STM investigation and Monte-Carlo modelling of spillover in a supported metal catalyst

A.J. Ramirez-Cuesta^{a,b,*}, R.A. Bennett^a, P. Stone^a, P.C.H. Mitchell^a, M. Bowker^a

^a Department of Chemistry, University of Reading, Reading, RG6 6AD, UK

^b Departamento de Física, Universidad Nacional de San Luis, Chacabuco y Pedernera, 5700 San Luis, Argentina

Received 17 May 2000

Abstract

Here we show, by in situ scanning tunnelling microscopy, that Pd nanoparticles enhance the rate of re-oxidation of a sub-stoichiometric TiO₂(1 1 0) surface. We believe that O₂ dissociatively adsorbs at 673 K on the Pd, and “spills over” onto the support where further reaction takes place. Tiⁿ⁺ interstitial ions in the bulk crystal lattice react with the spillover oxygen at the surface, preferentially growing TiO₂ around and over the particles. We employ a kinetic Monte-Carlo scheme to simulate this surface reaction and find a good correlation between the simulation and STM images. The simulation indicates that the surface structure may be reproduced in a model in which mobile species spillover from the metal particle, performs a random walk until it reaches a step edge where it may react (with low probability) to form TiO₂. The mobile species may also down-step to a lower terrace but up-stepping is forbidden. The temporal evolution of surface structures from both experiment and simulation are compared. © 2001 Elsevier Science B.V. All rights reserved.

Keywords: Monte-Carlo modelling; Spillover; Nanoparticles; TiO₂; Palladium; Oxygen

1. Introduction

The properties of nanoscale particles supported on surfaces, differ markedly from the bulk material due to their low-dimensionality [1,2]. Such alteration of physical and chemical properties is used in heterogeneous catalysis and gas sensing, where metal particles are spatially separated on a support material. The interaction between support and particle may also give rise to new chemistry due to the formation of new sites at the support/particle interface [3]. In addition, some reducible oxide supports creep-over and decorate the metal particles in reducing conditions. This

is most apparent for TiO₂ supported catalysts, where TiO_x species decorate particles resulting in a strong influence on the catalysis. The various effects resulting from this have been collectively termed the strong metal support interaction (SMSI) [4].

TiO₂ is used as a support or modifier in photocatalysis and catalysis, and as a sensing agent in gas sensors [5]. TiO₂ can appear in sub-stoichiometric (reduced) phases (as do other d⁰ transition metal oxides (V₂O₅, MoO₃ and WO₃)), and this has a marked effect upon electrical conductivity, chemical reactivity, and bulk and surface structure [6]. The cleaning of crystals for surface science studies in vacuum by sputtering and/or annealing results in reduction of the TiO₂ (accompanied by a colour change from pale yellow to blue). This reduction to form TiO_{2-x} is accommodated by the formation of Tiⁿ⁺ interstitial ions dissolved in

* Corresponding author.

E-mail address: a.j.ramirez-cuesta@reading.ac.uk (A.J. Ramirez-Cuesta).

the bulk. In real catalysts, metal particles can reduce the TiO₂ support by reaction in a reducing environment. During re-oxidation by an oxygen ambient we have shown [7], by imaging the reaction at high temperature, that the Tiⁿ⁺ interstitials are removed from the surface region of the crystal by incorporation into newly grown TiO₂ at the surface. This is indicated in the STM images by the nucleation and growth of (1 × 1) islands within the (1 × 2) terraces, and then to the formation of a second layer of (1 × 2) on the newly formed (1 × 1) islands. The reaction continues in a cyclic manner with alternating terminations of (1 × 1) and (1 × 2). On the basis of such a scheme, one may expect that nanoparticles residing on such a reacting surface may (i) be buried, (ii) form pits, or (iii) float as the TiO₂ grows around them. We have recently shown that the particles do indeed become covered by TiO₂, but the growth is preferential around the metal due to it acting as an enhanced source of oxygen atoms for the formation of TiO₂ [8,9].

The application of Monte-Carlo modelling to growth processes has led to a revolution in our understanding of this technologically important phenomenon, most notably in terms of scaling theory. Successful approaches to modelling rarely try to incorporate every last detail of the process, and generally a simplified model allows the essentials to be extracted. Here, we present a simple Monte-Carlo model for the spillover and growth, which reproduces the STM data well.

2. Experimental and methodology

Our model catalysts are prepared on a sputtered and vacuum annealed single crystal rutile TiO₂(1 1 0) surface to produce a clean surface with a (1 × 2) termination [10,11]. This termination and the colour change of the crystal (from white to dark blue) indicate a small departure from stoichiometry (TiO_{2-x}, $x < 10^{-4}$). Larger departures from stoichiometry show distinctive surface structures [8,12–14]. On this surface, we deposit Pd from high purity wire wrapped around a tungsten filament at 673 K and anneal at 773 K to produce stable particles with dimensions of approximately 30 Å width and 20 Å height. All images shown are taken at 673 K, and have a planar background subtracted but are otherwise unprocessed. Details regard-

ing the experimental chamber have been published elsewhere [15].

3. The Monte-Carlo simulation

The spillover process was simulated on a square lattice upon which a pre-set number of Pd particles were distributed at random. These particles were considered to be square in shape with a random distribution of linear sizes, varying from 10 to 14. The dissociation of O₂ is only allowed on the surface of such a particle. Once dissociated, each spillover atom starts a random walk on the surface (in this model, we consider that there is no interaction between diffusing particles). This simplification is valid because of the disparity between timescales in arrival rate of the gas molecules (10⁻⁷ mbar is approximately equivalent to 0.1 oxygen molecule–surface collisions per second per lattice site) and the diffusion process. Thus in the model, adsorption, diffusion and reaction events correspond to one timestep. During the diffusion process, the O atoms will have a probability P of reaction with a Ti interstitial coming from the bulk. If the atom is not at a step edge of TiO₂ nor the edge of a Pd particle, then $P = 0$; however, at TiO₂ step and particle edges the spillover atoms can react with probability $P = P_0$. This assumption is justified by the experimental observation of the rapid growth around the particle when compared with the bare surface by more than an order of magnitude, since we are trying to isolate the spillover effect we, therefore, choose $P = 0$ for adsorption at non-step sites. We also impose the following rule: an atom can step down to a lower terrace, but upstepping is forbidden. The reaction event leads to attachment of the atom at the edge and, therefore, growth of the terrace. The value of the parameter P_0 will determine the shape of the islands and the relative population of the growing layers. We considered the surface to have no defects or terraces prior to simulation, again in order to simplify the understanding of the process.

This 2 + 1 D model is related to the restricted ballistic deposition model in 1D in which growth can only be made at step sites and there is a biased random walk from a source site to a sink site [16,17]. The resulting 1D terrace morphology is a descending staircase of terraces from the source to sink site. We believe that the spillover process provides an essentially similar

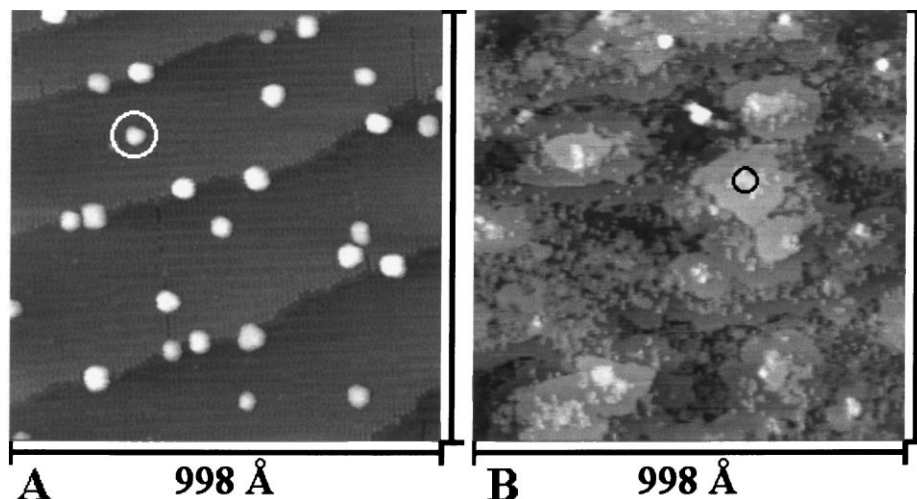


Fig. 1. (A) STM image showing the cross-linked (1×2) surface of $\text{TiO}_2(110)$ decorated with a low coverage of well dispersed Pd nanoparticles maintained at 673 K. (B) The same area after exposure to $\sim 90001 \text{ O}_2$ which significantly changes the surface morphology and results in the disappearance of the Pd particles. The circle in the images indicates the same particle. Images taken at 673 K, 1000 \AA^2 , 1 V and 0.1 nA.

mechanism to this and show in a sequence of snapshots (of both STM image and Monte-Carlo model) the resultant variation in surface structure of the re-grown TiO_2 .

4. STM results

Fig. 1A shows a low surface density of Pd nanoparticles distributed across the surface for which there appears to be some preference for decoration of step edges. The (1×2) reconstruction of the reduced surface is imaged between the particles [10]. Fig. 1B shows the same area of surface after exposure to $1 \times 10^{-7} \text{ mbar O}_2$ for 9300 s. The surface morphology has evolved to form raised islands on the originally flat terraces. It can be seen that these islands are centred on the original site of the Pd particles (see marker). The full sequence of 41 images between Fig. 1A and B can be found in [8].

Fig. 2A–F shows a higher density of larger particles also imaged in situ during the reaction of the Pd particles with $1 \times 10^{-7} \text{ mbar O}_2$ at 673 K, with Fig. 1A and B showing the surface just prior to oxygen exposure. In Fig. 2C, the reaction between interstitial Ti

and the O_2 has begun with the appearance of (1×1) islands forming around the particles, and a small number of short strings forming on the bare terraces [7]. In Fig. 2D, where the (1×1) islands have coalesced to form new terraces, new layers have begun to grow around the particles. However, in the regions relatively distant from the particles there is a reduced growth rate. This trend is continued in Fig. 2E where the (1×1) raised terraces surrounding the particles have spread and merged together, while areas far from the particles still show several monolayer (ML) deep pits. Fig. 2F shows that the terraces in which the Pd particles are now embedded have grown faster in regions of high particle density.

The physical mechanism by which the spillover occurs has been described recently [8,9], so will only be repeated briefly here. Oxygen readily dissociatively adsorbs on Pd surfaces in this temperature regime and so Pd particles, therefore, become a source of oxygen with which interstitial Ti can re-oxidise and grow. Crucially, the oxygen can diffuse off the Pd and onto the support and thus we find the rate at which the surface re-oxidises is ~ 16 times higher in the proximity of a Pd particle than for clean sub-stoichiometric TiO_2 [9].

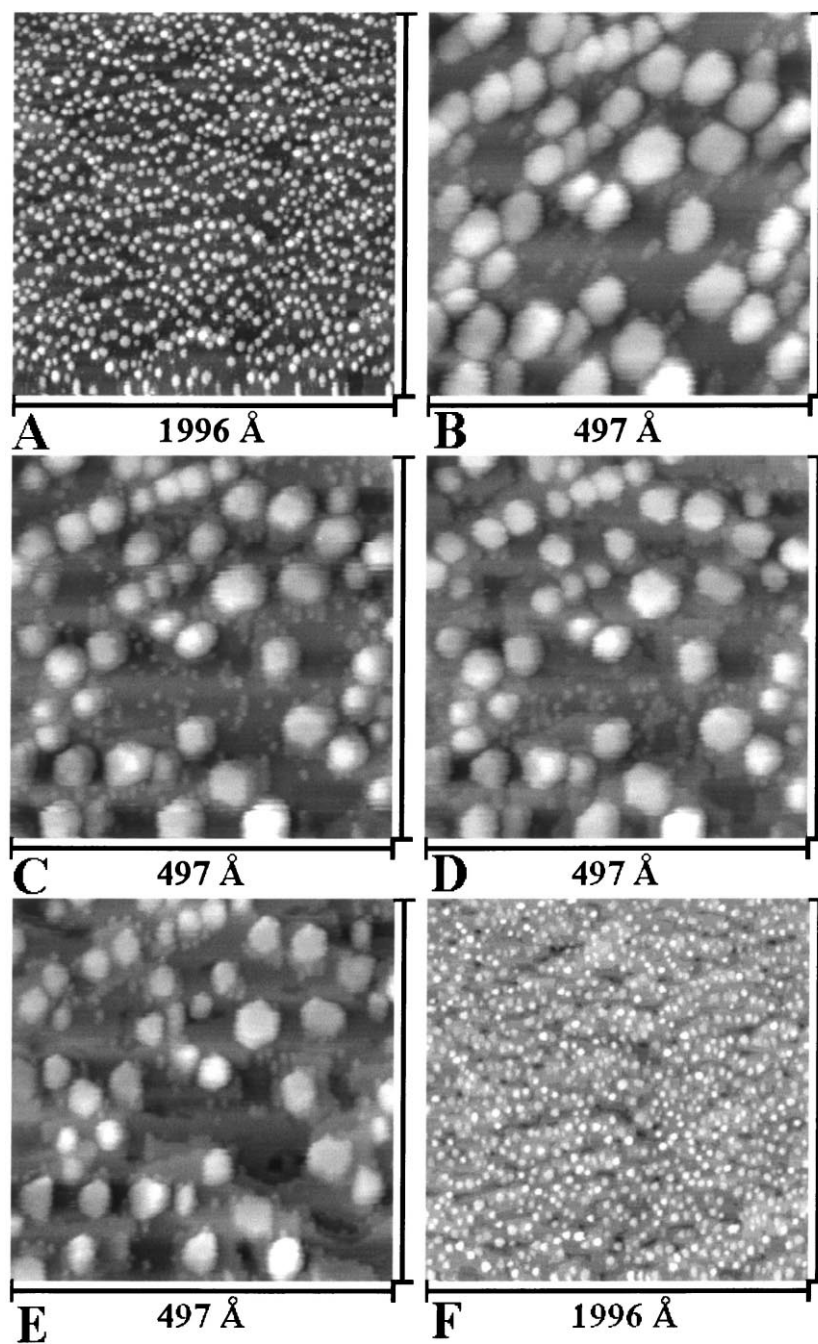


Fig. 2. The evolution of the surface during oxygen exposure. (A) A large area scan of the surface decorated to a high density with Pd nanoparticles. (B)–(E) Evolution of the TiO₂ surface surrounding the Pd particles at high resolution; terraces are nucleated at the particles and extend laterally across the surface with time and eventually merge. (F) Morphology of the surface that develops with raised terraces predominantly forming in regions with a high cluster density. All images taken at 673 K, 1 V and 0.1 nA.

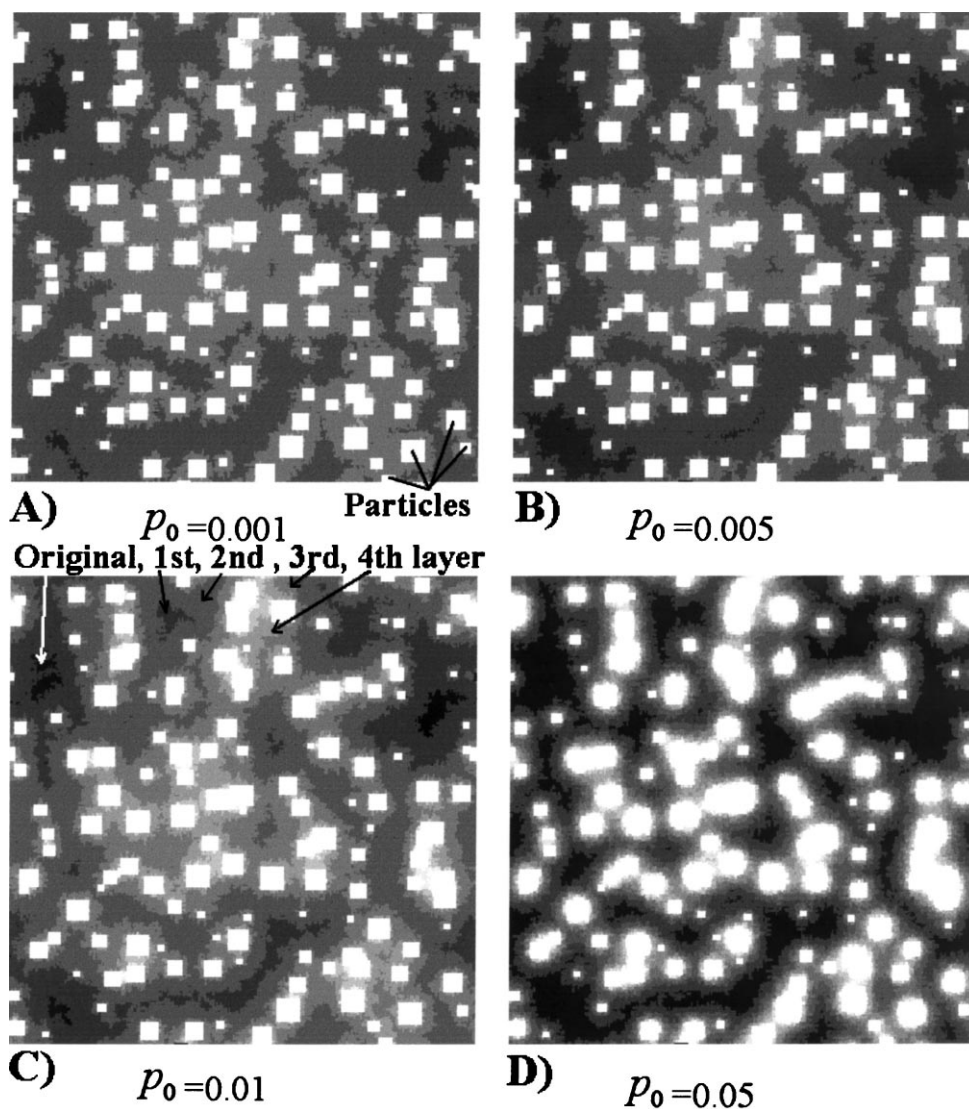


Fig. 3. The surface morphology resulting from simulations with differing values P_0 (reaction probability at a step edge). (A) and (B) With low reaction probability, the near complete growth of a monolayer across the surface with subsequent layers growing close to the particles. (C) and (D) With high reaction probability, the initial layer does not grow to completion and the particles show strongly enhanced growth at their boundaries. All simulations were run for a constant coverage of ~ 3 ML. Images are 512×512 lattice sites with periodic boundaries.

5. Simulation results

Fig. 3 shows snapshots taken at the end of the simulation in which three monolayers of oxygen were deposited on the surface via the spillover mechanism described earlier for different values of parameter P_0 . P_0 represents the probability for a spillover species to

become attached to a step edge. In Fig. 3A, the low value of $P_0 = 0.001$ gives a relatively flat surface with limited nucleation at the model Pd particles. The results for $P_0 = 0.005$ shown in Fig. 3B, show a similar morphology. The entire TiO_2 surface has grown by at least one monolayer with an enhanced level of growth in regions with locally higher density of Pd.

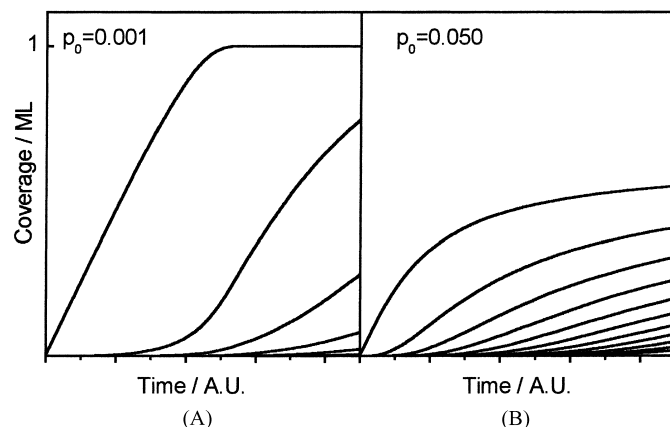


Fig. 4. The growth of successive layers as a function of time for two limiting values of the reaction probability P_0 . (A) Initial layer growing near to completion before the second layer nucleates and grows, subsequent layers grow at slower and slower rates. (B) First layer does not grow to completion as multiple terraces grow simultaneously with increasing frequency and decreasing rate.

Simulating with the value of P_0 at 0.01 leads to the pronounced growth localised at the Pd particle with regions remote from the Pd particles showing no growth (Fig. 3C). In the extreme case of $P_0 = 0.05$ (Fig. 3D) re-growth is restricted to the immediate vicinity of the particles with the appearance of large interconnected areas with no growth at this coverage.

6. Comparison and discussion

6.1. Time evolution of terraces

Fig. 4 shows the time evolution of the TiO_2 layer-by-layer growth, in the form of fractional areas covered versus simulation time, for the limiting cases of low and high P_0 values. For $P_0 = 0.001$, the first TiO_2 monolayer grows to near completion before nucleation of the next layer at the particle starts. The initial rate of growth of the first layer is constant in time, whereas subsequent layers show variable rates of growth with a slow build up to a constant rate which then begins to slow as new layers are nucleated. At the other extreme, $P_0 = 0.05$, the initial layer does not grow to cover the entire surface and the nucleation of subsequent layers occurs rapidly producing multiple co-existing growing terraces. These terraces also show the variable growth patterns, however, the time at which each terrace begins to develop becomes successively shorter such that growth rates

of all terraces become slower. Physically, this leads to the terraces becoming bunched.

Due to the nature of the STM imaging and the presence of pre-existing surface steps, direct extraction of terrace areas as a function of time is problematic. However, we have managed to measure the area of growth, around each Pd particle shown in Fig. 1A, as a function of time until the terrace grows out of the field of view of the STM. The results, at 673 K, are shown in Fig. 5 in a similar manner to those extracted from the simulation, and indicate that the first layer of growth

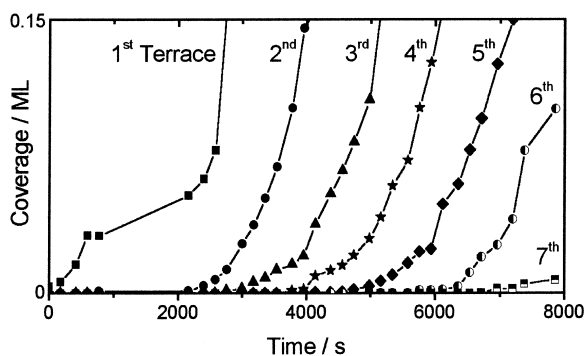


Fig. 5. The rate of growth of terraces extracted from STM images acquired during growth. The initial terrace grows at constant rate for an extended time period with subsequent layers growing more frequently showing good correlation with the simulation for low reaction probability ($P_0 \sim 0.001$ – 0.005).

initially occurs for a long time period before growth of the subsequent layers. These subsequent layers then begin to grow in rapid succession, each at a rate that increases with time. However, the later the terrace begins to grow (i.e. the higher the terrace), the slower the overall rate of growth of that terrace. These characteristics are well reproduced in the model system with low values of $P_0 = 0.001$ – 0.005 .

6.2. Morphology of final surface

To evaluate the morphology of the resultant surface in both experiment and simulation, we have employed a height–height correlation function, related to each

particle's centre, to determine the morphology as a function of distance from the particle. The correlation function is defined as

$$G(\mathbf{r}) = \langle (z(\mathbf{r}_0 + \mathbf{r}) - z(\mathbf{r}_0))^2 \rangle$$

where $z(\mathbf{r})$ is the height at position \mathbf{r} , and \mathbf{r}_0 the position of the particles. We have calculated this function centred on the metal particles in order to extract the growth behaviour from the simulations and STM images in a comparable manner. Length scales in the simulation are scaled to give the correct interlayer (Z) distance of 3.2 \AA per step. However, the radial distance cannot be scaled as such due to the anisotropy in real surface structure, which we have purposely avoided

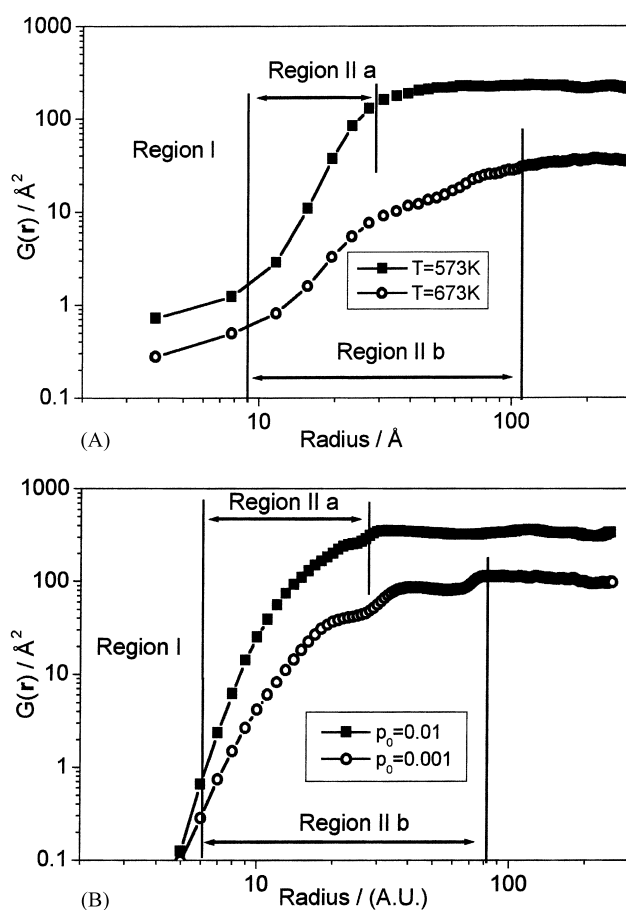


Fig. 6. Height–height correlation function for different temperatures in the experiment and different probabilities P_0 in the simulation. Region I corresponds to the particle self-correlation, regions IIa and IIb show the length scale over which the growth of terraces are correlated. Note the undulation at lower temperature arising from the long inter-terrace separation.

simulating for clarity, hence r corresponds to units of the Monte-Carlo lattice.

Fig. 6A shows the $G(r)$ averaged over several particles for the spillover induced growth at two temperatures, 573 and 673 K. At 573 K and in region I, there is close correlation which corresponds to the radius of the particle. Region IIa contains the information on the step edges that are bunched up around the particle and extends only to around 30 Å radius. Beyond this range, the surface morphology is no longer correlated with the particle position, and the function tends to a limiting value dominated by the difference between initial particle height and the height of the surrounding terrace far from the particle. As growth at low temperatures is restricted to the particle vicinity, this value is high. At 673 K, the initial region I is comparable to that at 573 K due to similar particle sizes. However, region IIb extends to ~ 100 Å, and shows some undulating structure due to extended terrace formation. Again for large r , the plot goes to a limiting value which at this temperature is slightly lower than at 573 K due to the growth of the terrace between particles. Some fine structure is apparent in this large r region, which is due to islands and terraces forming around neighbouring particles.

The simulation results (Fig. 6B) show broadly similar trends in the limiting value and region II, if we relate P_0 to the experimental temperature. For high probabilities of sticking at the step edges ($P_0 = 0.01$), there is a steep and smooth increase in $G(r)$ in region IIa, indicating the growth of large number of bunched steps. This is similar to the low temperature growth process. Conversely, low probabilities ($P_0 = 0.001$) behave more like the high temperature result with structure developing due to the formation of extended terraces. Again, the correlation lengths of region II for the differing values of P_0 are significantly different. In region I, $G(r) = 0$ because in the simulation the particles are modelled as cubes (i.e. with constant Z over the particle).

The simulation shows an increased tendency for concentration of growth around the particles with increasing P_0 . Similar traits may be seen in experiments in which the surface temperature is varied. At low temperature (573 K) growth is concentrated around the particles, whereas at higher temperatures (673 K) there is markedly less growth at the particle periphery [8]. However, other factors may also need to be taken

into account such as temperature dependent sticking probability on the Pd (and desorption again at high temperatures); further work in both experiment and simulation is required (and ongoing) to differentiate these and other factors.

7. Conclusion

We have shown by scanning tunnelling microscopy that metal particles enhance the re-oxidation of reducible support materials by dissociative chemisorption of oxygen molecules which generate oxygen atoms that spillover onto the surface of the support. Interstitial Ti^{n+} ions are removed from the bulk and react with the oxygen to form a new surface layer. The nanoparticle enhanced removal of Ti^{n+} from the bulk by this mechanism is ~ 16 times faster than on the clean surface. Many layers of TiO_2 may grow during re-oxidation such that the metal particles are buried. A model has been developed and simulated within the Monte-Carlo framework in which the spillover species leaves the metal particles and diffuses on the oxide terraces until encountering a step edge. The step edges (including the metal particle-oxide interface) are reactive sites at which a new TiO_2 unit may be grown. The simulation reproduces well the surface morphology and rate of terrace growth if the spillover species is allowed to react with low probability only at step edges and upstepping of mobile species is forbidden.

Acknowledgements

The authors wish to thank the EPSRC for funding.

References

- [1] M. Valden, X. Lai, D.W. Goodman, *Science* 281 (1998) 1647.
- [2] C.P. Vinod, G.U. Kulkarni, C.N.R. Rao, *Chem. Phys. Lett.* 289 (1998) 329.
- [3] F. Bocuzzi, A. Chiorino, S. Tsubota, M. Haruta, *J. Phys. Chem.* 100 (1996) 3625.
- [4] S.J. Tauster, *Acc. Chem. Res.* 20 (1987) 389.
- [5] R.M. Walton, D.J. Dwyer, J.W. Schwank, J.L. Gland, *Appl. Surf. Sci.* 125 (1998) 187, 199.
- [6] V.E. Henrich, P.A. Cox, *The Surface Science of Metal Oxides*, Cambridge University Press, Cambridge, 1996.

- [7] P. Stone, R.A. Bennett, M. Bowker, *New J. Phys.* 1 (1999) 8, www.njp.org.
- [8] R.A. Bennett, P. Stone, M. Bowker, *Faraday Discuss.* 114 (1999) 267, movie available at www.rsc.org/is/journals/current/faraday/fd999114.htm.
- [9] R.A. Bennett, P. Stone, M. Bowker, *Catal. Lett.* 59 (1999) 99.
- [10] C.L. Pang, S.A. Haycock, H. Raza, P.W. Murray, G. Thornton, O. Gülseren, R. James, D.W. Bullett, *Phys. Rev. B* 58 (1998) 1586.
- [11] R.A. Bennett, P. Stone, N.J. Price, M. Bowker, *Phys. Rev. Lett.* 82 (1999) 3831.
- [12] G.S. Rohrer, V.E. Henrich, D.A. Bonnell, *Science* 250 (1990) 1239.
- [13] R.A. Bennett, S. Poulston, P. Stone, M. Bowker, *Phys. Rev. B* 59 (1999) 10341.
- [14] R.A. Bennett, *Phys. Chem. Commun.* (2000) 3, www.rsc.org/ej/qu/2000/B001938K/index.html.
- [15] M. Bowker, S. Poulston, R.A. Bennett, P. Stone, A.H. Jones, S. Haq, P. Hollins, *J. Mol. Catal. A: Chem.* 131 (1998) 185.
- [16] H. Park, M. Ha, I.-M. Kim, *Phys. Rev. E* 51 (1995) 1047.
- [17] M. Ha, H. Park, M. den Nijs, *J. Phys. A: Math. Gen.* 32 (1999) L495.